ACOUSTIC TRANSDUCERS AND LENS DESIGN FOR ACOUSTIC MICROSCOPY

C-H. Chou and B. T. Khuri-Yakub

Edward L. Ginzton Laboratory
W. W. Hansen Laboratories of Physics
Stanford University
Stanford, California 94305

INTRODUCTION

The transducer-lens system is one major component in the performance of an acoustic microscope. The design criteria for the various types of applications of an acoustic microscope are different. For surface imaging applications, it is desired to have a small spot size and low sidelobe level. For materials characterization and subsurface imaging applications (such as subsurface crack imaging), it is required to have high surface wave excitation efficiency. Several researchers addressed the problem of surface imaging.[1-5] Also, some work has been done to investigate materials properties indirectly by using so-called V(z) curves.[6-8] The resolution obtained in the latter case is always much worse than that of the corresponding lens. The direct measurement of surface wave velocity by using conventional transducer-lens systems also gives poor spatial resolution because it suffers from the interference of the specularly-reflected signal with the surface wave component caused by the low efficiency of surface wave excitation.[9] In order to increase the surface wave excitation efficiency, we first modified the design of the standard longitudinal transducer-lens system. Furthermore, we worked out a novel configuration, i.e, the shear transducer-lens system. This gives very high surface wave excitation efficiency and anisotropic acoustic beam distribution. Therefore, it can be used for direct measurements of materials properties in different directions with much less defocus than in the case of conventional transducer-lens systems. This gives the potential of many new applications of materials characterization with excellent spatial resolution.

LONGITUDINAL TRANSDUCER-LENS SYSTEM

A typical transducer-lens system is schematically depicted in Fig. 1. For surface imaging applications, the acoustic beam generated by the longitudinal transducer propagates through the buffer rod and is focused at the surface of the sample. In order to obtain a low sidelobe level, the buffer rod length is chosen to correspond to $S = 1$ where

$$S = \lambda l/a^2 \tag{1}$$

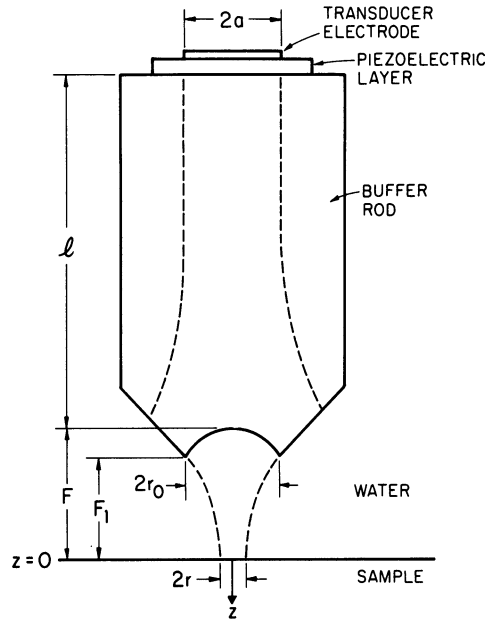

Fig. 1. Schematic diagram of typical transducer-lens system.

where λ is the wavelength of the longitudinal wave in the buffer rod, l is the length of the buffer rod, and a is the radius of the transducer.

Bringing the lens closer to the sample (defocusing) induces surface acoustic waves, which give quantitative information about the materials properties, such as surface wave velocity and residual stress. Therefore, it is very important to excite surface waves efficiently for materials characterization. To evaluate the efficiency of surface wave excitation, we will look at the impulse response of the transducer-lens system in the time domain.

The theoretical calculation of the time domain response of a transducer-lens system is described in reference 10. Figure 2a shows the theoretical result of the time domain response of a longitudinal transducer-lens system with the buffer length corresponding to $S = 1$ at the center frequency of 50 MHz when defocused -1.8 mm . The diameter of the lens is 4.5 mm and the F-number is 1.65. The sample is hot pressed silicon nitride. It is clear that the received signal consists of the specularly-reflected signal, which comes first, and the surface wave component, which arrives second, and that the surface wave signal is weaker than the specularly-reflected signal. Figure 2b shows the corresponding experimental result which agrees with the theoretical result very well.

In order to increase the relative amplitude of the surface wave signal, it would be helpful to minimize the acoustic illumination at the center region of the lens. One way to do this would be to place the lens in the near field of the transducer, at a location where the on-axis field strength is at a minimum, such as for $S = 0.5$.

Figures 3a and 3b show the theoretical and experimental results for the time domain response of a longitudinal transducer-lens system that we constructed with a buffer length corresponding to $S = 0.6$, a center

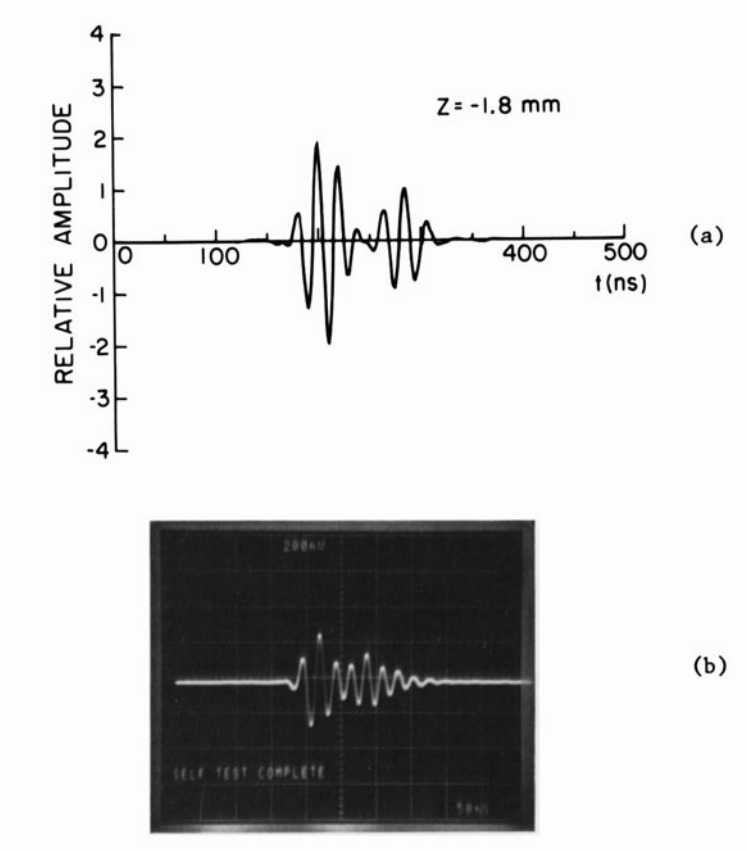

Fig. 2. The time domain response of a longitudinal transducer-lens system. S = 1 at f_0 = 50 MHz , Z = 1.8 mm , Lens Diameter = 4.5 mm , F-number = 1.65 , Sample: Si_3N_4. (a) Theoretical. (b) Experimental.

frequency of 40 MHz , and a defocusing distance of -1.8 mm . The lens diameter is 3.5 mm , the F-number is 1.65 , and the sample is also hot pressed Si_3N_4. The surface wave excitation efficiency, with respect to the specular reflection, in this case has been increased by about 12 dBs compared to that of the transducer-lens system of Fig. 2.

SHEAR TRANSDUCER-LENS SYSTEM

A new configuration of a transducer-lens system is a shear transducer-lens system. In this case, we use a shear polarized transducer on the buffer rod instead of the longitudinal transducer. The shear wave propagates through the buffer rod to the lens-water interface and is mode converted into a longitudinal wave in the water. Since the incident angle at different locations of the interface varies, the longitudinal transmittance is a function of r/F , where r is the radial distance from the center of the lens, and F is the focal length of the lens. Figure 4 shows the theoretical calculation of the transmittance function at the lens-water interface of a shear transducer-lens system with a buffer rod of fused quartz.[11] In this calculation, we assume that the transducer is radially polarized and the lens is in the far field of the transducer so that the incident shear wave is uniformly distributed. Considering the transmittance function as the equivalent lens illumination, we calculated the time domain response as we did for

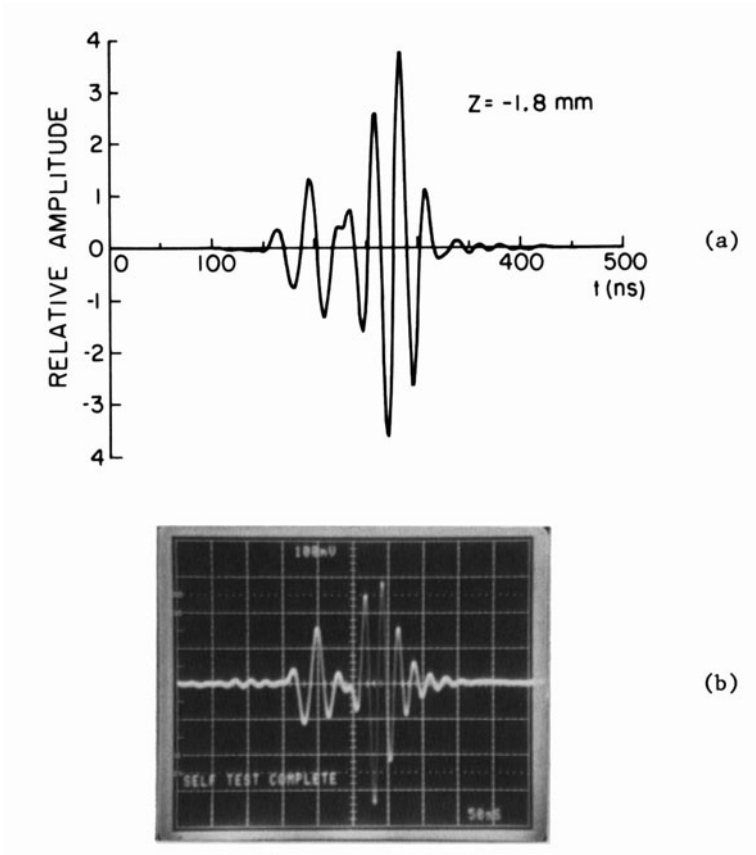

Fig. 3. The time domain response of a longitudinal transducer-lens system. S = .6 at f_0 = 40 MHz , Z = -1.8 mm , Lens Diameter = 3.5 mm , F-number = 1.65 , Sample: Si_3N_4. (a) Theoretical. (b) Experimental.

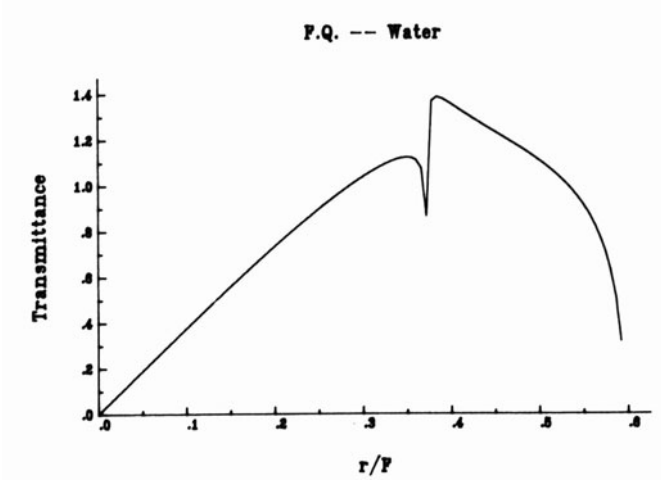

Fig. 4. Transmittance at lens-water interface of a shear transducer-lens system. Buffer: fused quartz.

the longitudinal transducer lens. The result is shown in Fig. 5 for a shear transducer-lens system with defocusing of -1.8 mm operating at a center frequency of 50 MHz . The diameter and F-number of the lens are 2 mm and 1.65 , respectively. The sample is still hot pressed Si_3N_4.

Figure 5 shows clearly that the specularly-reflected signal is negligible compared to the surface wave component in this case. This allows us to obtain a clean surface wave with little defocusing, which is very important for materials characterization with high spatial resolution as we will see in the next session.

In practice, it is easier to construct a linearly-polarized shear transducer. Figure 6 shows the theoretical result of the acoustic field distribution in the aperture plane for a linearly-polarized shear transducer-lens system. It can be seen that the acoustic field is anisotropic in this case.

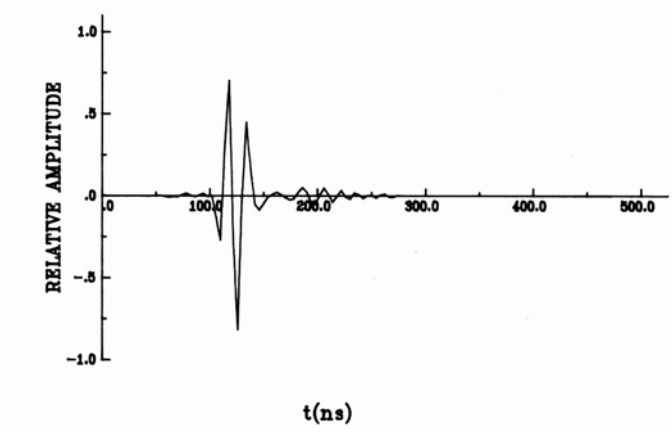

Fig. 5. The theoretical time domain response of a radially-polarized shear transducer-lens system. f_0 = 50 MHz , Z = -1.8 mm , lens diameter = 2 mm , F-number = 1.65 , Sample: Si_3N_4.

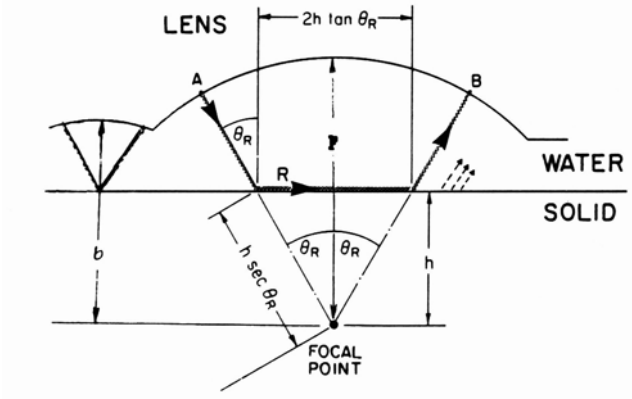

Fig. 6. Theoretical result of acoustic fields distribution in an aperture plane of a linearly-polarized shear transducer-lens system.

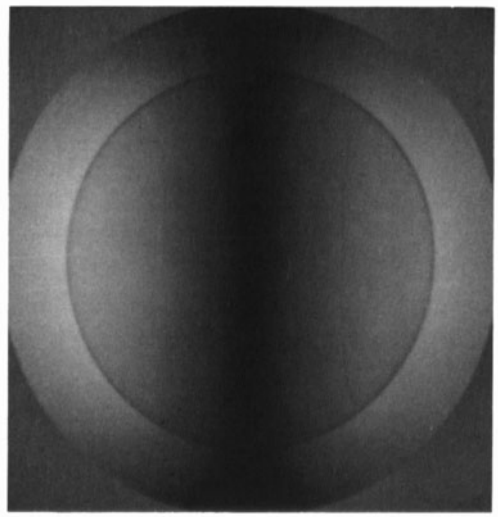

Fig. 7. Schematic diagram of the configuration of a lens for the surface wave velocity perturbation measurement by a shear transducer-lens system.

APPLICATIONS

To take advantage of the "clean" surface wave excitation and the anisotropic property of the shear transducer-lens system, many novel applications can be expected, such as measuring the surface wave velocity, residual stress, and anisotropy of materials as well as film thickness, and subsurface crack depth with good spatial resolution. Here we will give some examples of the potential applications of the shear transducer-lens system.

In order to measure the surface wave velocity of materials, a reference signal is needed. Figure 7 shows the schematic diagram of the configuration of the lens for surface wave velocity perturbation measurement. In this configuration, we introduced a cylindrical lens with weak focusing to provide a reference signal. It is designed to focus at the surface of the sample when the main lens is defocused by -1.5 mm . The F-number of this cylindrical lens is 2.5 . The corresponding focal depth is 0.67 mm at 50 MHz . The maximum half-angle of the lens is below the Rayleigh angle of the samples we will work with. Therefore, the received signal by this lens has no surface wave component.

By using this configuration, we measure the phase change of the signal received by the main lens with respect to the signal received by the cylindrical lens. The phase variation caused by the surface wave velocity perturbation along the sample can be expressed by[11]

$$\Delta\phi = 2\omega h(\Delta V_R/V_R)\tan\theta_R/V_R \qquad (2)$$

where V_R is the surface wave velocity and θ_R is the Rayleigh angle of the sample. Therefore, if we measure the phase change, we will be able to determine the surface wave velocity perturbation.

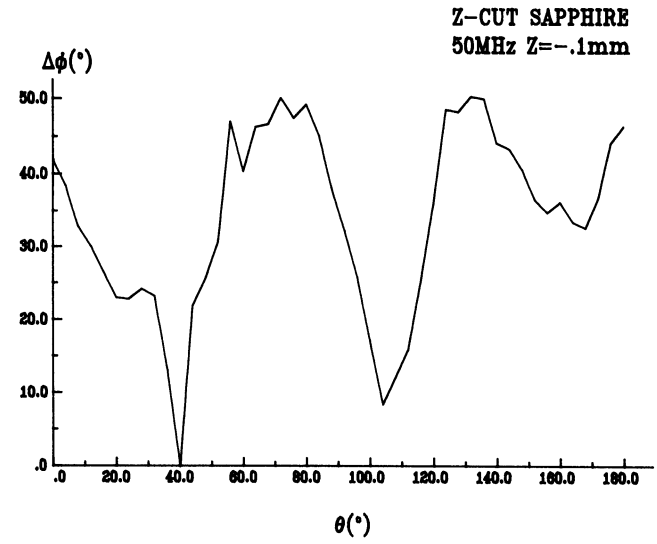

(a)

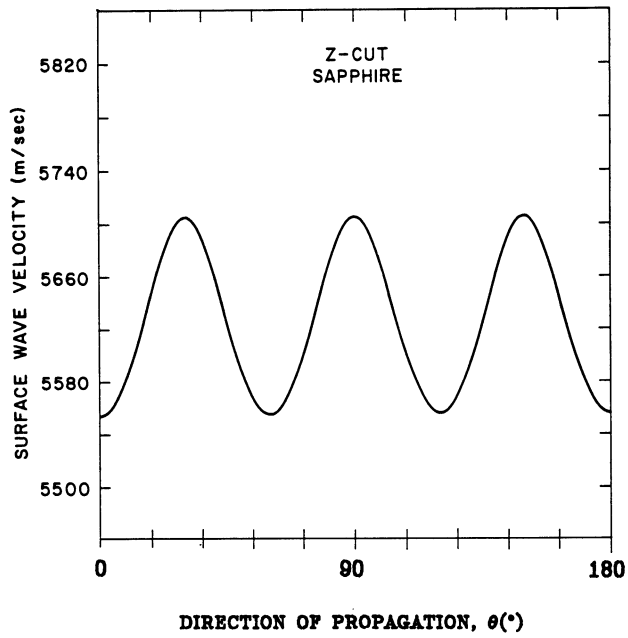

(b)

Fig. 8. (a) Measured slowness curve of Z-cut sapphire by a shear transducer-lens system with a defocus of .1 mm . (b) Theoretical prediction of the surface wave velocity slowness curve of Z-cut sapphire.

Figure 8a shows the preliminary results of the surface wave velocity slowness curve measurement of a Z-cut sapphire sample by the shear transducer lens, as described above. The operating frequency is 50 MHz . The defocusing distance is -.1 mm . Figure 8b is the theoretical prediction. The experimental result shows the six-fold crystal symmetry which is in agreement with theory.

Figure 9 shows the measured phase change across a gold film step with a thickness of 2000 Å deposited on a glass substrate by the same transducer-lens system at 50 MHz with a -.2 mm defocusing distance.

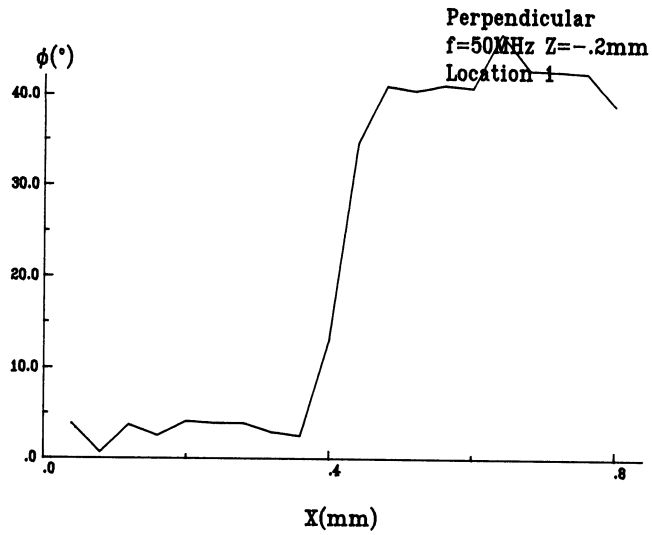

Fig. 9. Measured phase change along a film step by a shear transducer-lens system with a defocus of .2 mm. Sample: glass substrate with deposited 2000 Å Au film.

The theoretical phase change due to the existence of the film is 43' , which agrees with the experimental result of 39' very well. The spatial resolution is .1 mm in this case, which is 3.3 λ in water.

CONCLUSION

We have developed both a longitudinal transducer-lens system and a shear transducer-lens system for providing high efficiency of surface wave excitation. The novel configuration of the shear transducer-lens system makes us able to measure surface wave velocity in different directions with good resolution, which is very useful for materials characterization. The work presented here is still preliminary. There is much work to be done for improvement. Many applications are expected.

ACKNOWLEDGMENT

This work is supported by the Department of Energy under Contract No. DOE DE-FG03-84ER45157.

REFERENCES

1. C. F. Quate, A. Atalar, and H. K. Wickramasinghe, Proc. IEEE 67, 1092-1113 (1979).
2. A. J. Miller, "Applications of Acoustic Microscopy in Semiconductor Industry," in Acoustical Imaging, Vol. 12, 67-78 (Edited by E. A. Ash and C. R. Hill, Plenum Press, NY, 1982).
3. F. Faridian, Proc. IEEE Ultrasonics Symp., 759-762 (1985).
4. M. Nikoonahad and E. A. Ash, Proc. IEEE Ultrasonics Symp., 557-560 (1984).
5. A. Atalar, "Acoustic Reflection Microscope," Ph.D. Dissertation, Stanford University (1978).

6. K. K. Liang, G. S. Kino, and B. T. Khuri-Yakub, IEEE Trans. on Sonics & Ultrasonics SU-32, 213-224 (1985).
7. J. Kushibiki and N. Chubachi, IEEE Trans. on Sonics & Ultrasonics SU-32, 189-212 (1985).
8. C-H. Chou and G. S. Kino, "The Evaluation of V(z) in a Type II Reflection Microscope," accepted for publication, IEEE. Trans. on UFFC (1986).
9. K. K. Liang, "Precision Phase Measurement in Acoustic Microscopy," Ph.D. Dissertation, Stanford University (March 1985).
10. C-H. Chou, B. T. Khuri-Yakub, and G. S. Kino, "Lens Design for Acoustic Microscopy," accepted for publication, IEEE Trans. on UFFC (1986).
11. B. A. Auld, Acoustic Fields and Waves in Solids, Vol. 2, Chapter 9 (John Wiley & Sons, NY, 1973).